DIGITAL CONTROL OF A STEPPING MOTOR

by

DONALD FRANCIS ZELLER

B.S., University of Notre Dame
1965

SUBMITTED IN PARTIAL FULFILLMENT OF THE
REQUIREMENTS FOR THE DEGREE OF
MASTER OF SCIENCE

at the

MASSACHUSETTS INSTITUTE OF TECHNOLOGY
September, 1966

Signature of Author _____
Department of Electrical Engineering, September 30, 1966

Certified by _____
Thesis Supervisor

Accepted by _____
Chairman, Departmental Committee on Graduate Students

DIGITAL CONTROL OF A STEPPING MOTOR

by

DONALD FRANCIS ZELLER

Submitted to the Department of Electrical Engineering on September 30, 1966, in partial fulfillment of the requirements for the degree of Master of Science.

ABSTRACT

Special driving circuitry was designed and tested to increase the maximum pulsing rate of a Superior Electric Slo-Syn stepping motor. Theoretically, this circuitry should extend the maximum pulsing rate from 200 pps to 2000 pps by reducing the electrical lag due to the inductance of the motor winding. However, due to mutual coupling between the windings and the mechanical parameters of the motor, the maximum rate was limited to 450 pps.

Included in this design were logic schemes for pulsing the motor continuously or in bursts and for reversing the motor. The experimental results consisted of oscillograms of the winding current and angular output. These traces demonstrated the effects of coupling and the mechanical parameters.

Thesis Supervisor: George C. Newton, Jr.
Title: Professor of Electrical Engineering

ACKNOWLEDGEMENT

The author expresses his sincerest thanks to Prof. G. C. Newton, Jr. for suggesting the thesis topic and advising him during the experimental work. He is especially indebted to Prof. Newton for his encouragement during the most difficult period of the research. Thanks are also due to the author's roommate, Mr. Vincent Schirf, and to his brother, Mr. John R. Zeller, for their ideas and time in assisting with the experimental work. Finally, an expression of gratitude is due to the personnel of the Electronic Systems Laboratory, especially Mrs. Grace Mitchell and Mrs. Ionia Lewis for their assistance in the typing and the preparation of this thesis.

CONTENTS

LIST OF FIGURES

LIST OF FIGURES (Continued)

LIST OF TABLES

CHAPTER I

INTRODUCTION AND STATEMENT OF PROBLEM

1.1 BACKGROUND

Modern control systems operate with digital signals since this provides the most efficient and fastest transmission of information. As such, system designers find it difficult to use conventional actuators since they are analog devices and require some digital-to-analog converters in the system. Also, it is usually the mechanical lag inherent in these actuators which limits the high-speed performance of the over-all system. However, their mechanical output is a necessary stage in most systems, so there is a definite need for an electro-mechanical device with the power output capability but which operates on digital signals with minimum response time.

The stepping motor is a device which has properties suitable for these purposes. It is inherently a digital-analog converter since it translates digital data into analog position with exact synchronism between pulses and angular motion. The stepping motion is equivalent to sequentially pulsing a series of coils arranged in a circle at a definite stepping angle.[1] The reaction between the stator field and the permanent magnet rotor or soft iron core, depending on which type of magnetic detent is used, causes the indexing action. This is demonstrated in Fig. 1.1.[1]

The distinguishing feature of the stepping motor is the magnetic detent action. When the rotor indexes from one position to the next, the inertial effect causes an oscillation about the new null position. The magnetic reaction between the two fluxes causes a holding action which damps

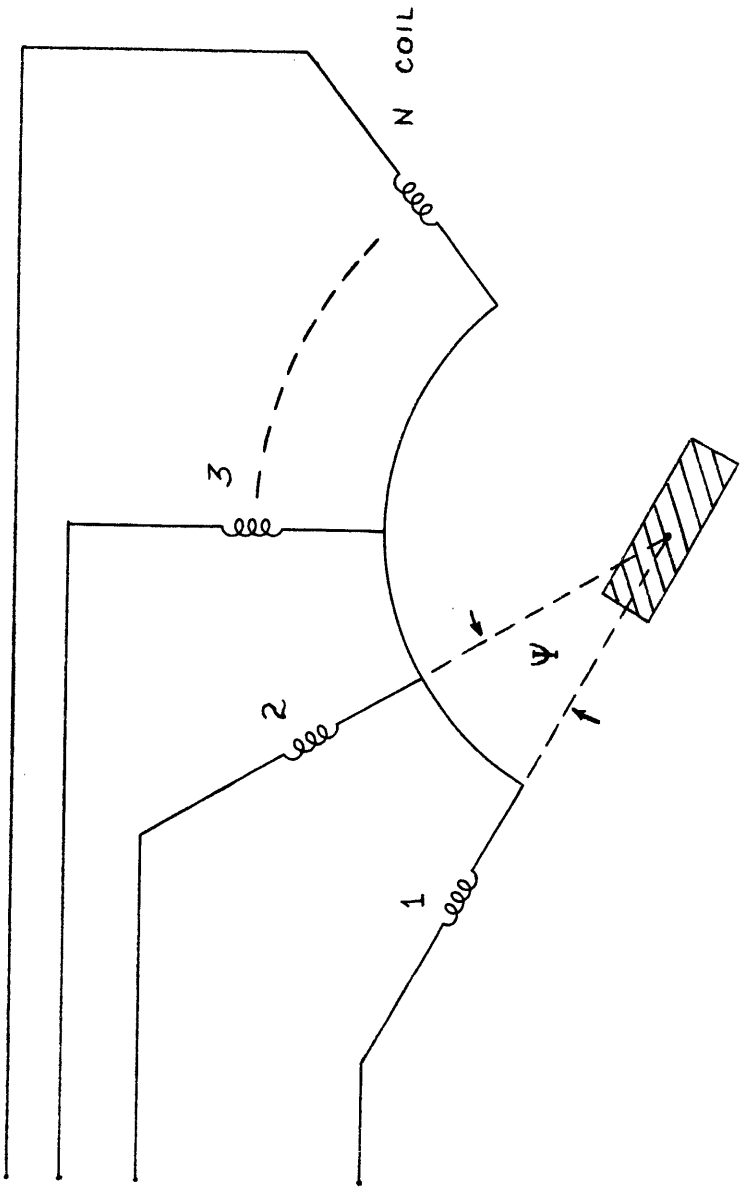

Figure 1.1 Stepping Motor Analog

this oscillation. The effect is equivalent to a second-order feedback positioning system during each step.[2] With this scheme the rotor locks in more rapidly than under the frictional damping of the conventional motor. Since these are discrete positions determined by the motor design, together with this magnetic damping, the stepper provides a fast, accurate, and incremental output which is applicable to digital systems.

1.2 SLO-SYN MOTOR

The Superior Electric Slo-Syn stepping motor is one of the class of magnetically detented steppers. That is, torque is developed as a result of the interaction between a rotating magnetic field caused by applying d.c. pulse excitation to the stator windings in a four-step sequence and an undirectional flux, produced by a permanent magnet rotor. The design is referred to as a synchronous inductor motor.

In order to understand the operation of the motor,[3] it is necessary to explain its construction. Refer to Fig. 1.2.[3] The stator has eight poles. There are two stator windings, with four poles per winding. For motor type SS150-1010 the stator windings are bifilar. That is, the two windings are center-tapped to give four different flux paths. However, the center-tapped windings are wound on the same poles so there are still four poles per winding. Both the stator and rotor have a toothed periphery. The stator teeth are at a pitch of 48 teeth for 360^{o}, although there are only 40 teeth, one tooth per pole being omitted to allow space for the windings. Rotor teeth are at a pitch of 50 teeth for 360^{o}. The rotor itself is a permanent magnet, which is magnetized axially. It has two separate disks with the same number of teeth but offset by one half a rotor tooth-pitch. The torque due to the two sections of the rotor add directly. This

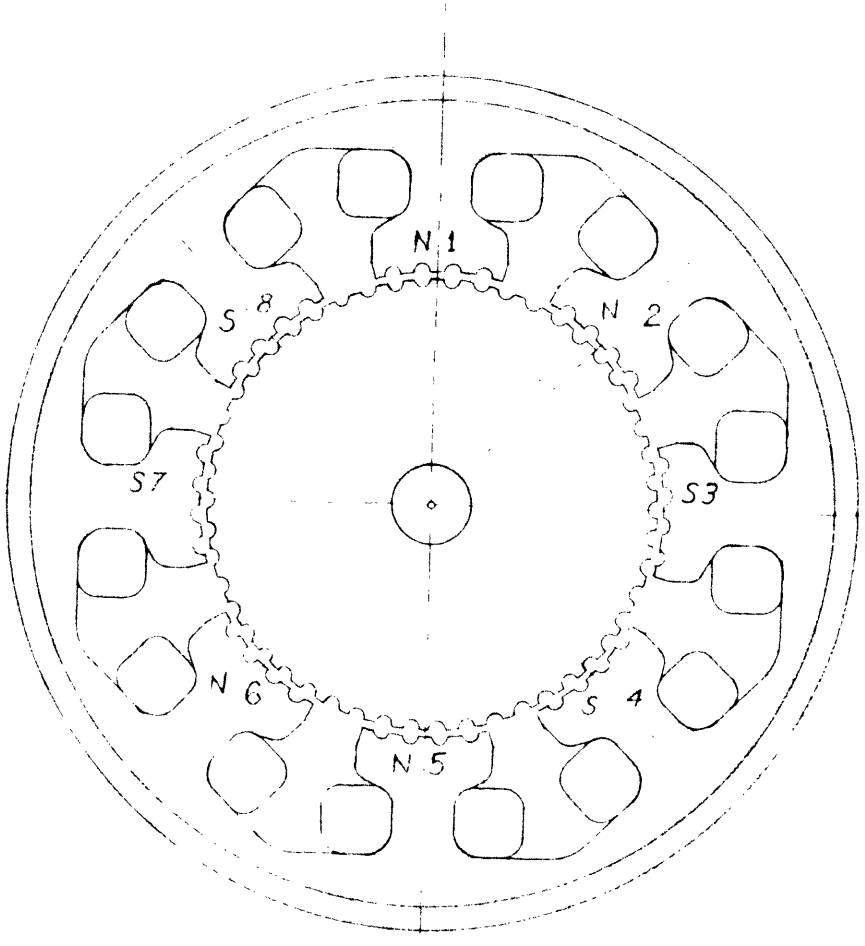

Figure 1.2 Cross Section of Synchronous Inductor Motor Perpendicular to Shaft

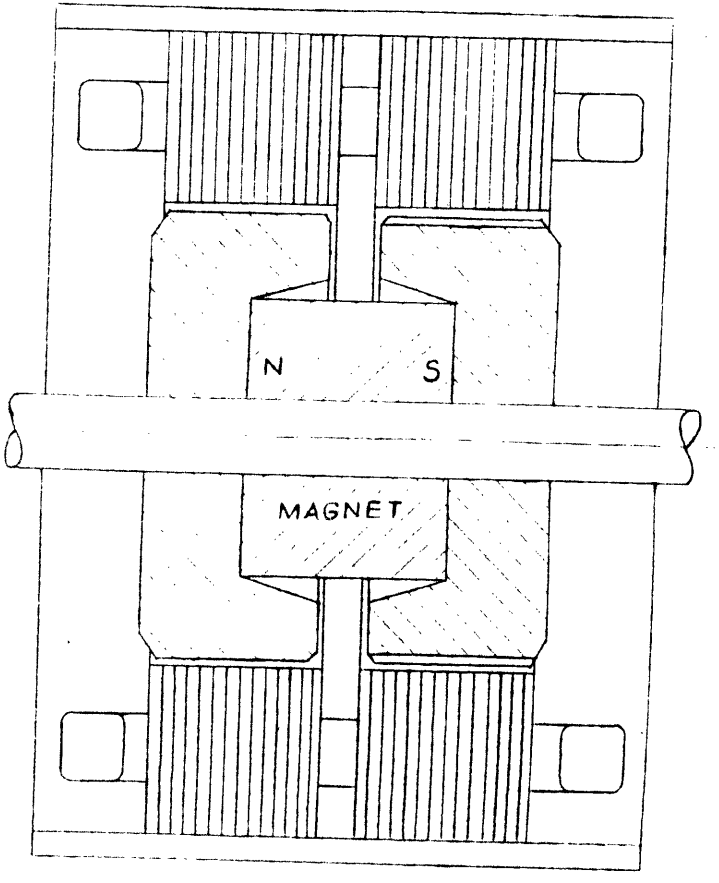

Figure 1.3 Cross Section Parallel to Shaft

DRAWING IS NOT TO SCALE

construction is shown in Fig. 1.3.[3] Also indicated is the path of the undirectional flux due to the magnet.

For the motor in Fig. 1.2, four switching operations are required to advance the rotor one tooth-pitch. With 50 teeth on the rotor, 200 switching operations are needed for a complete revolution. Thus, each step is an increment of 1.8°. These switching operations will be discussed in Chapter II.

1.3 PURPOSE AND METHOD OF INVESTIGATION

The purpose of this experimental investigation is to determine the limitations of the motor's transient behavior and to improve the device's response characteristics. That is, in standard operation, the Slo-Syn SS150 motor has a maximum pulsing rate of 200 pulses per second. The rate is limited by both the electrical and mechanical time constants inherent in the motor. This investigation concentrated on an attempt to reduce the affective electrical time constant of the windings by special driving circuit techniques. These techniques are simplified for the SS150 motor since it has bifilar windings.[5] Instead of reversing the current in a winding, current of the same polarity is switched to a winding wound in the opposite direction. Thus only a single-ended power supply is needed.

The results of employing these techniques are best demonstrated in the output torque vs speed curves. As the switching rate is increased the currents cannot attain their steady state values due to the inductance in the windings. Thus the output torque is reduced as the stepping rate increases. A typical graph for a standard two-winding motor is shown in Fig. 1.4. With the bifilar windings, only half the winding space is utilized, reducing the total flux linkages. Therefore, the output torque is

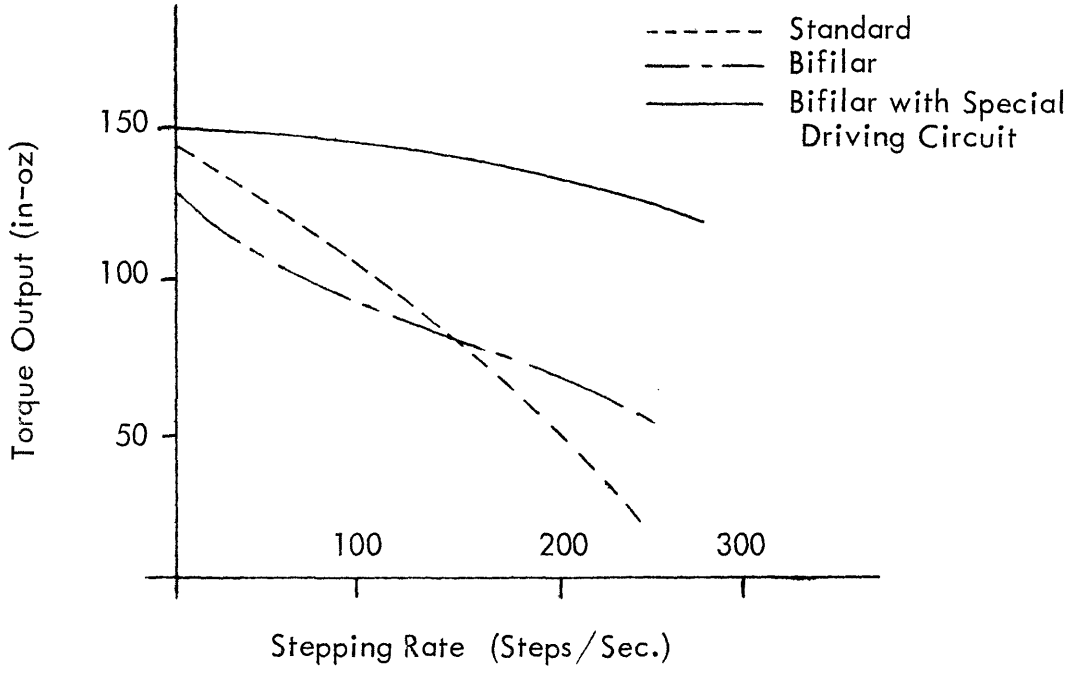

Figure 1.4 Torque vs Speed Characteristics

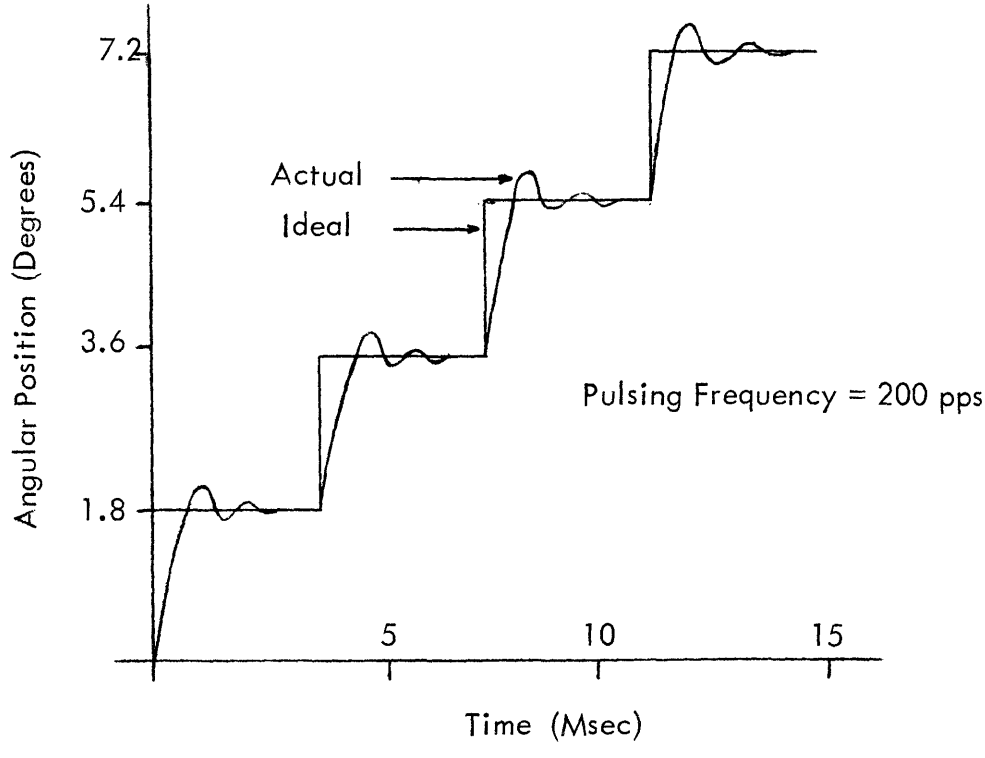

Figure 1.5 Angular Response

reduced. However, the electrical time constant is decreased since a small wire size is used. This improves the slope of the output torque vs stepping rate curve. This effect is indicated in Fig. 1.4 also.

With the special driving circuit, which reduces the electrical lag to a constant, small value over an entire frequency range, the desired output torque vs stepping rate curve is shown in Fig. 1.4. This assumes the accelerating torque and frictional torque are constant over this range of frequencies.

Ideally speaking, the maximum pulsing can be extended to a value whis is limited by the reduced electrical lag. However, the mechanical lag, caused by the inertia and friction of the rotor must also be considered. That is, the ideal position vs time curve is shown in Fig. 1.5. However, the actual step response shown in Fig. 1.5 shows a delay and oscillation, due to the mechanical parameters of the motor. Therefore it is possible for the mechanical lag to limit the maximum pulsing rate, depending on its value relative to the improved electrical time constant.

Finally, this research will demonstrate the effect of mutual coupling between the windings. Since some of the windings are wound on the same poles, the coupling is nearly 100 percent between them. Therefore any transient behavior has an opposing effect in the coupled winding. Thus the driving circuit design must compensate for this phenomenon. These results are explained and analyzed in Chapters III and IV.

CHAPTER II

ELECTRICAL CIRCUITRY FOR THE SYSTEM

2.1 INTRODUCTION

Figure 2.1 is a general block diagram of the over-all system for driving the motor. The Slo-Syn motor (type SS150-1010) as described in Chapter I, is a digital-to-analog converter which has one output step for each input pulse. However, the motor is not a device which steps automatically as soon as d.c. excitation is applied to its windings. There is a definite sequence of excitation which results in proper stepping. This chapter will treat the theory and fabrication of the intermediate stage circuitry which interconnects the pulse generator and the output stages that drive the motor.

2.2 LOGIC CIRCUITRY FOR UNIFORM PULSING

For uniform stepping, a simple logic arrangement of three flip-flops provides the proper sequence of excitation to the motor windings. This logic scheme is shown in Fig. 2.2. The flip-flops were Fairchild micrologic elements (number 923). Also, it was found that these devices would not operate properly unless the triggering pulse width was less than one fourth the pulsing period. The waveforms for this logic are shown in Fig. 2.3. Since the driving stage is essentially an amplifier for the logic output, this scheme provides an "on-off" sequence of excitation to the motor windings.

To demonstrate how the motor operates with this command logic, a simplified four-position stepping motor will be used, represented in

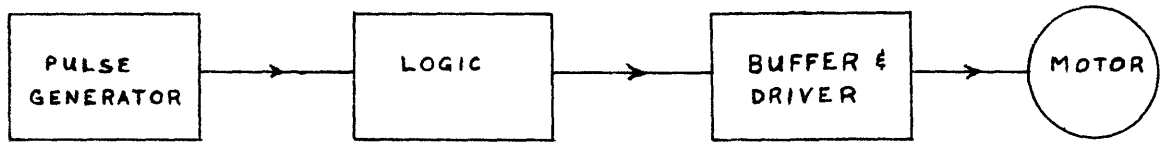

Figure 2.1 Block Diagram of System

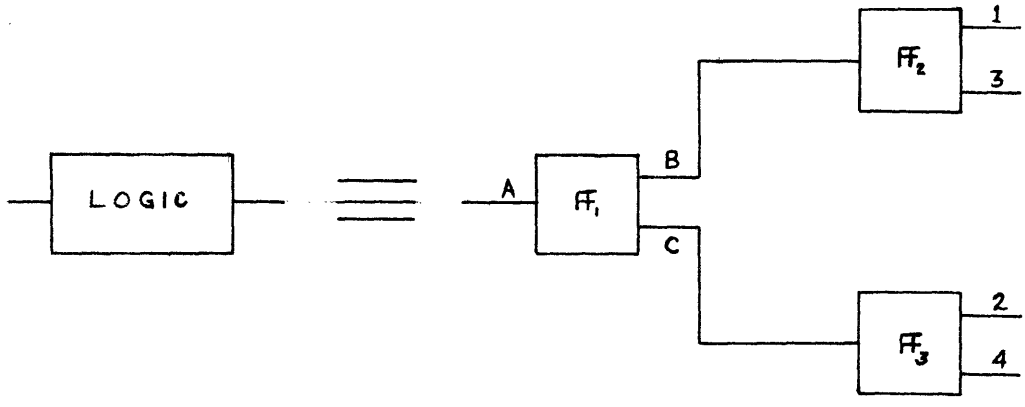

Figure 2.2 Uniform Pulsing Logic

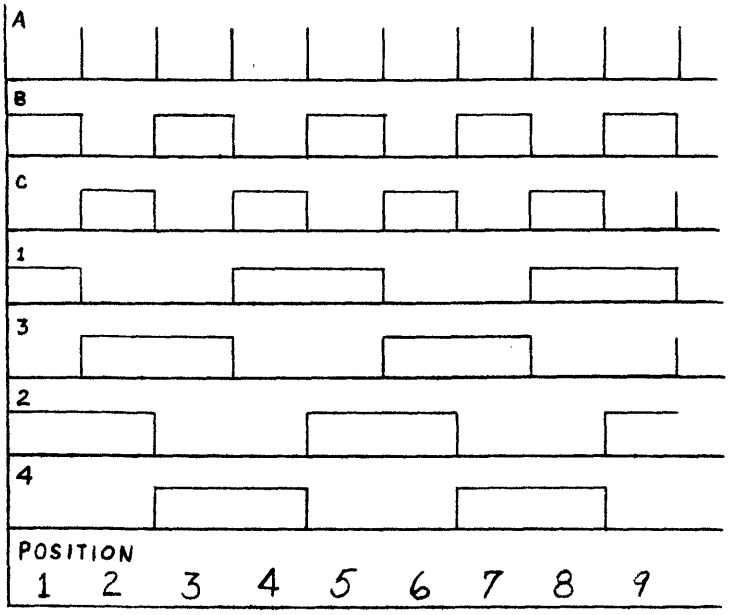

Figure 2.3 Waveforms for Uniform Pulsing Logic

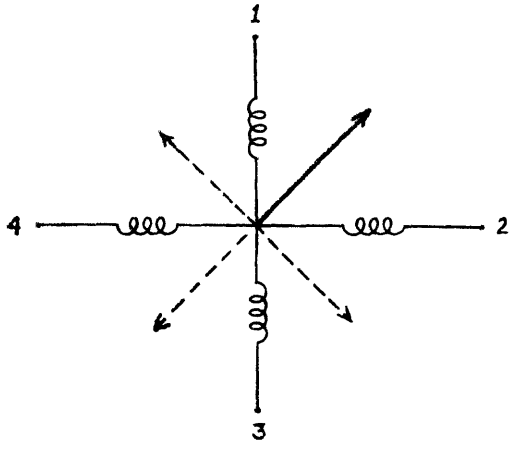

Figure 2.4 Schematic Diagram of Stepping Motor

	WINDINGS			
POSITION	1	3	2	4
1	+	−	+	−
2	−	+	+	−
3	−	+	−	+
4	+	−	−	+
1	+	−	+	−

Table 2.1 Step Sequence for Uniform Pulsing

Fig. 2.4 by four windings. (The bifilar Slo-Syn motor also has four different flux paths.)

In Fig. 2.4 the arrow represents the rotor position. Figure 2.3 shows that FF_2 and FF_3 change state alternately with each input pulse. In this way the excitation to the windings is switched in an overlapping manner as shown in the table in Fig. 2.4. Thus the motor steps from one position to the next with each input pulse. The direction of rotation is arbitrary depending on the initial states of the flip-flops. This basic principle applies as well to a multi-step motor such as the Slo-Syn SS150-1010.

2.3 LOGIC CIRCUITRY FOR PULSE PACKETS

Included in the circuit design for this research were logic schemes for non-uniform pulsing and reversing the motor. Although these are mainly intended for further experimentation, it is important to explain their operation fully.

Shown in Fig. 2.5 is the block diagram for pulsing the motor continuously with groups of pulses at various frequencies and with a varying number of pulses in a group. This logic scheme involves a single gating operation which interrupts the pulse train for the period of the monostable.[7] The monostable is triggered by the output of the electronic counter. This is a CMC Model 786C Dual Pre-set counter which is capable of a variety of counting operations. For this operation it simply counts the number of input pulses to a pre-set number, triggers the one-shot and recycles after the NOR gate is cleared. The inverter and NOR gate were implemented with Fairchild 914 micrologic dual input gates. The monostable circuit has a 1.2 second period. Thus, all transient behavior had ceased before another

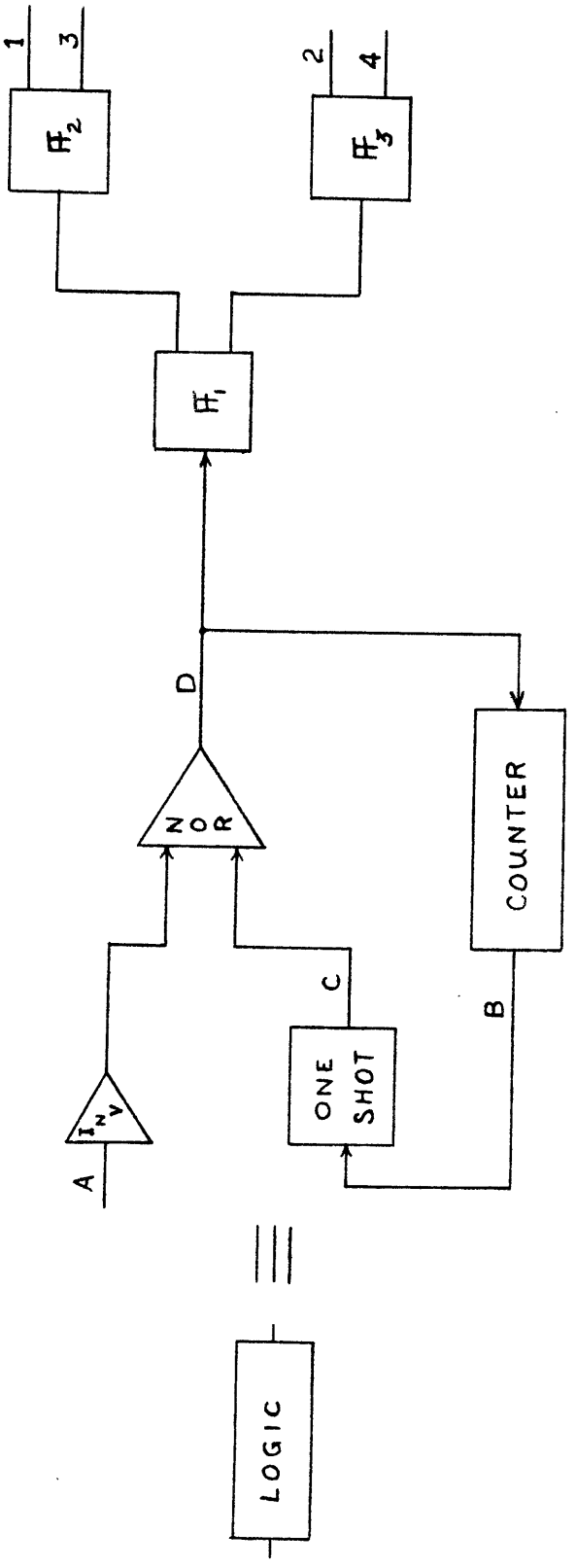

Figure 2.5 Logic Scheme for Pulsing Motor in Bursts

packet of pulses was applied. To demonstrate this operation, the waveforms for a packet of five pulses are shown in Fig. 2.6.

2.4 LOGIC CIRCUITRY FOR REVERSING THE MOTOR

The reversing process is best explained by referring to the uniform pulsing operation. Here the sequence of excitation is accomplished by having FF_2 and FF_3 toggle alternately with each input pulse. Also, the position of the motor changes with each toggling action, as shown in Table 2.1. Referring to Table 2.2, it is seen that the sequence of positions is reversed if the state of the motor windings is maintained for a single input pulse. This is accomplished by blocking a single triggering pulse to either FF_2 or FF_3 while FF_1 toggles once, as shown for pulse number 4.

A logic scheme which accomplishes this process is shown in Fig. 2.7. For this scheme the dual count mode of the CMC counter is used, since it is necessary to trigger FF_4 twice each cycle. Again, Fairchild micrologic elements were used for this logic. However, this method is not perfect since it assumes definite initial states of FF_1 and FF_4. Shown in Fig. 2.8 is one possible set of waveforms for this logic scheme. To demonstrate what happens if FF_1 is in its complementary state, shift the pulse in waveform D ahead one input pulse period. Following the NOR operation, FF_2 will have an extra triggering pulse. If FF_4 is in its complementary state, then the "off-on" portions of waveform D are reversed and only a single triggering pulse reaches FF_2 during a cycle. This ambiguity of operation can be avoided by using the preset mode on FF_4 and making a symmetrical NOR operation for the triggering pulses to FF_3.

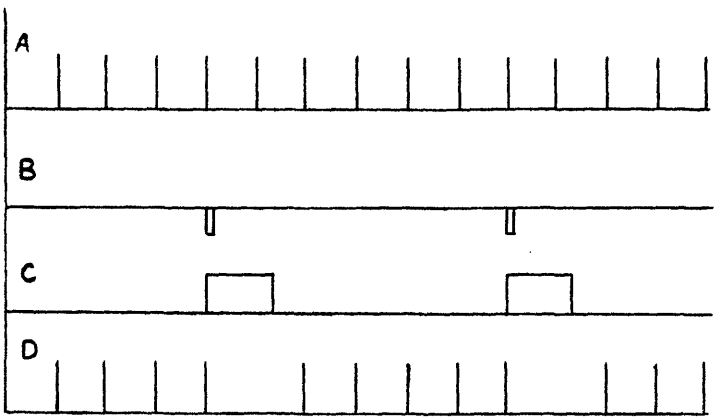

Figure 2.6 Waveforms for Pulse Packet Logic

				Windings			
INPUT PULSE	FF1	FF2	FF3	1	3	2	4
1	SW		SW	+	−	+	−
2		SW		−	+	+	−
3			SW	−	+	−	+
4				−	+	−	+
5			SW	−	+	+	−
6		SW		+	−	+	−
7			SW	+	−	−	+
8	↓	SW		−	+	−	+

Table 2.2 Step Sequence for Reversing Operation

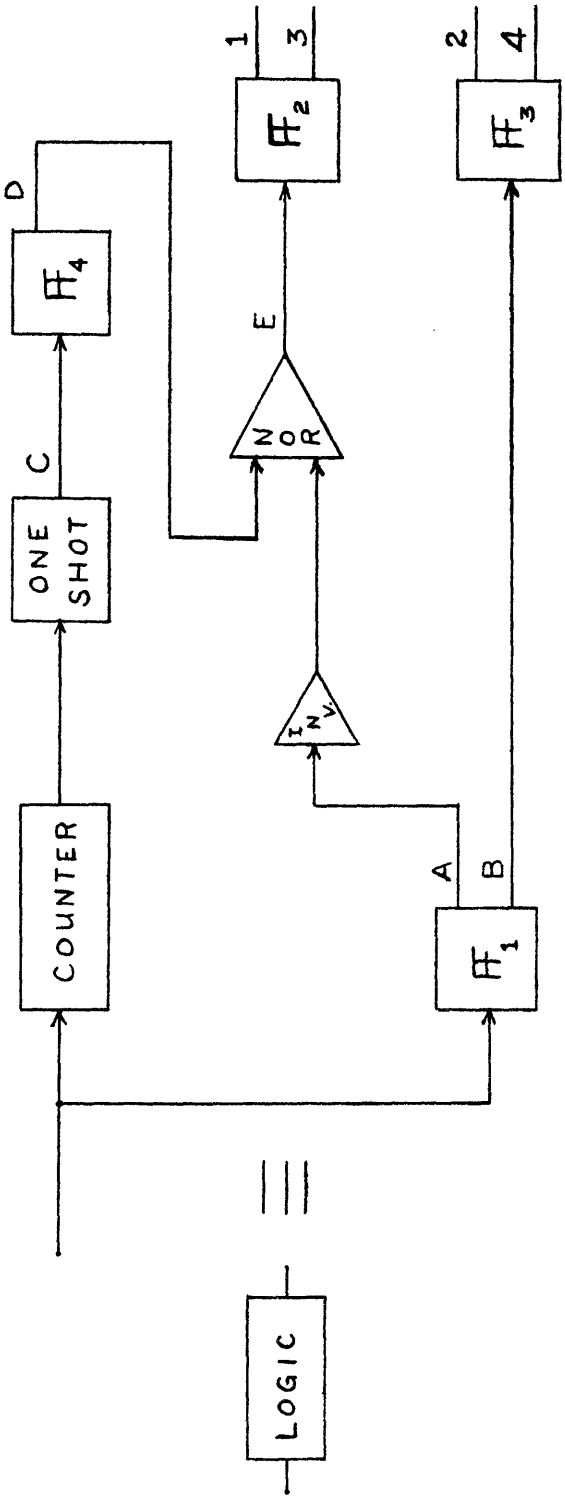

Figure 2.7 Logic Scheme for Reversing Motor

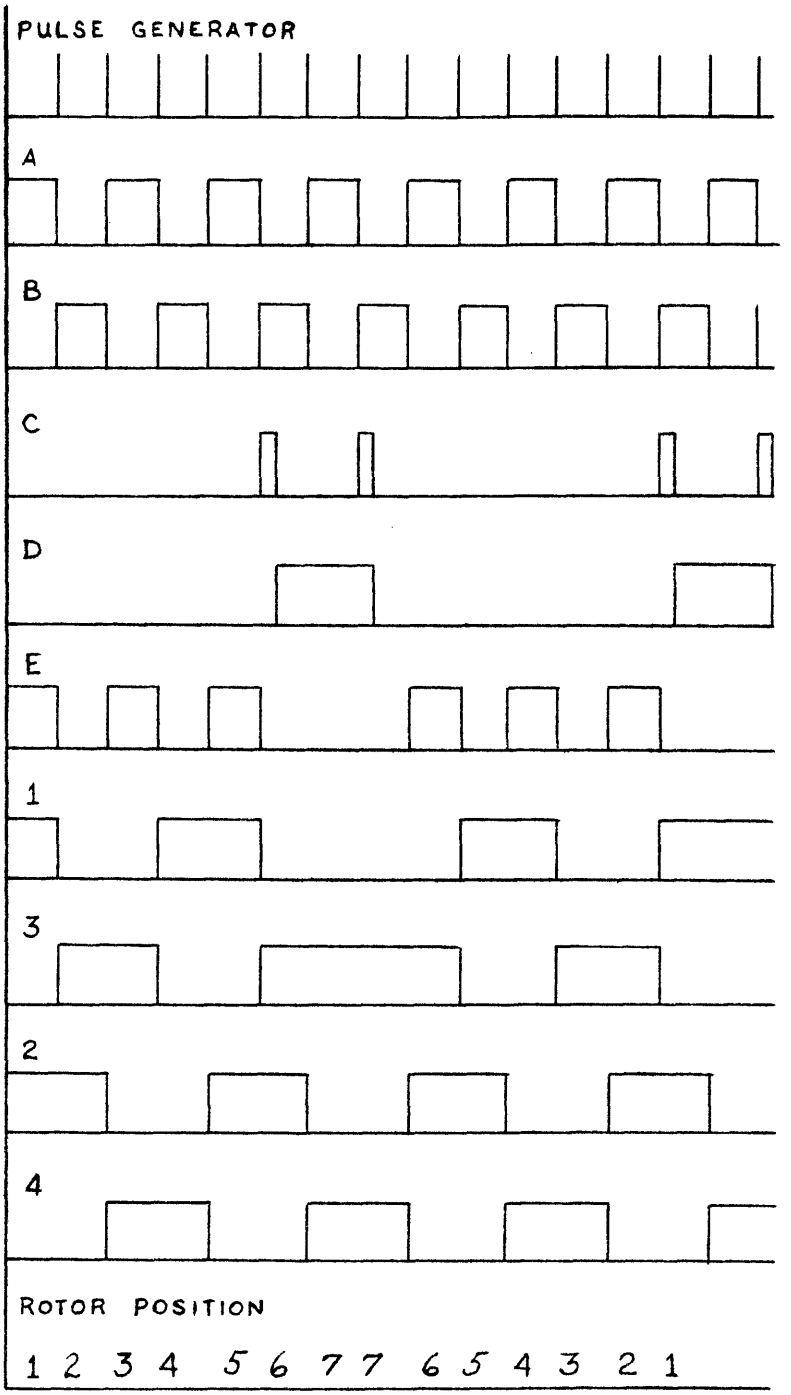

Figure 2.8 Waveforms for Reversing Logic

2.5 DRIVING CIRCUITRY

The driving stage is composed of three parts: forward gain, turn-off path, and spiking circuit. The forward gain is a standard design and is essentially an amplifier for the low micrologic output. The power amplification needed to drive the motor windings at rated values (10 volts, 1.25 amps) is achieved using Delco DTS 423 transistors. Amplification of the low micrologic output for the power transistors is provided by a single inverter stage. This circuitry is shown in Fig. 2.9.

The major part of this research was devoted to designing the turn-off path for the winding currents. Its main purpose was to provide a path for the current during turn-off and to reduce the lag in current decay caused by the inductance of the winding, thereby increasing the maximum pulsing rate. Also, without this path, turning off the DTS 423 transistor causes very large induced voltage spikes at its collector, given by $L \frac{di}{dt}$. Power dissipation and mutual coupling between the windings were the major design considerations.

The initial design involved a simple resistor-diode path. Since the DTS 423 acts as an "on-off" switch, the equivalent circuit for a single winding is shown in Fig. 2.10. When the switch opens excitation to the winding L ceases and the current stored in the winding decays exponentially to zero through the resistor path. The time of this exponential decay is determined by the L/R ratio: the larger R the faster the decay. Theoretically, with a value of 300 Ω, the L/R ratio was reduced enough to achieve pulsing rates up to 2000 pps. (The winding itself has an inductance of 30 mh and resistance of 8 Ω.) That is, the electrical time constant, τ, for this decay is 0.1 msec. The pulsing period T should be greater than 5τ to insure

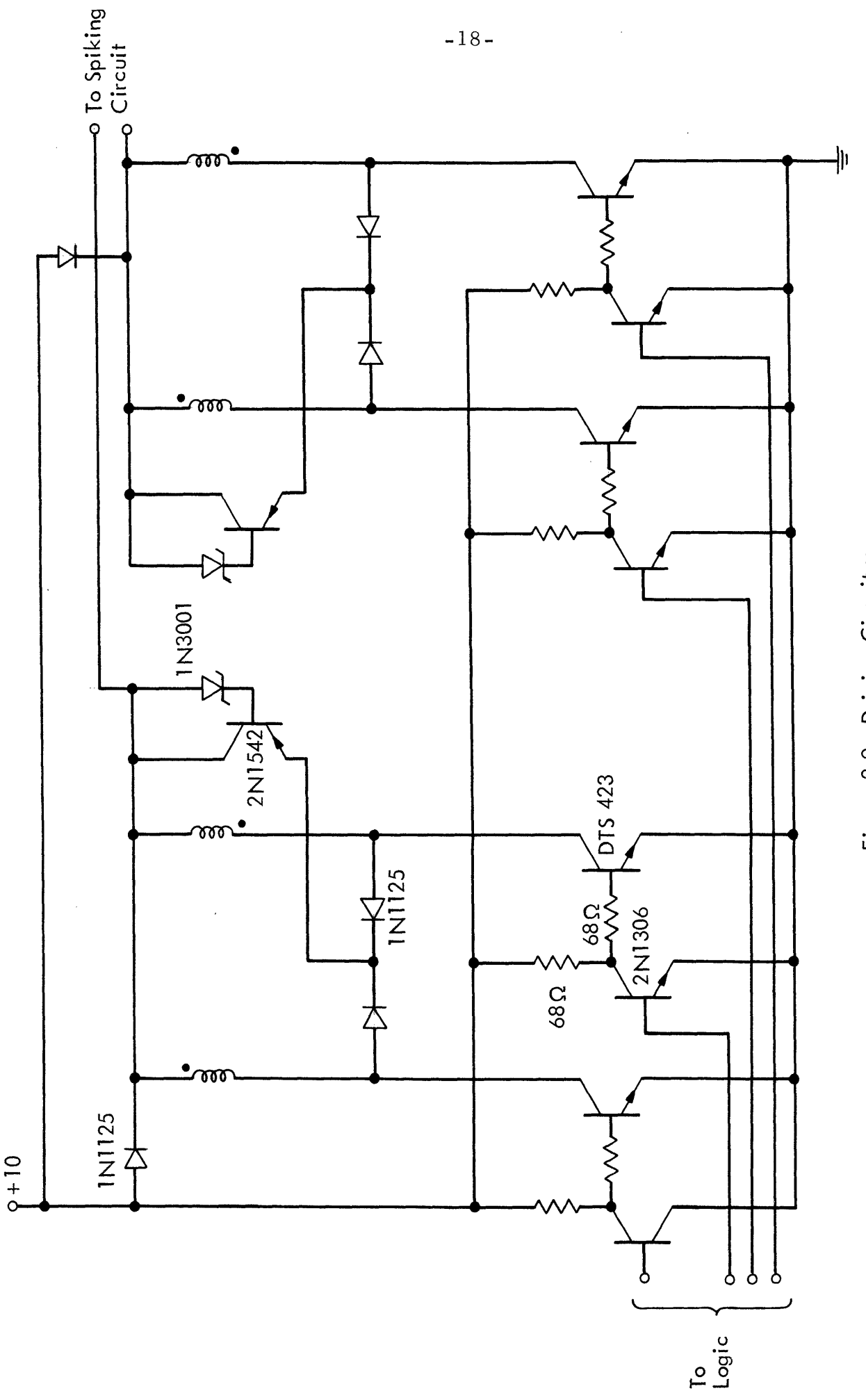

Figure 2.9 Driving Circuitry

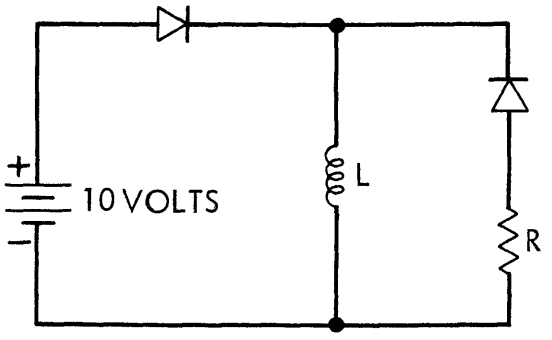

Figure 2.10 Equivalent Circuit of Single Output Stage

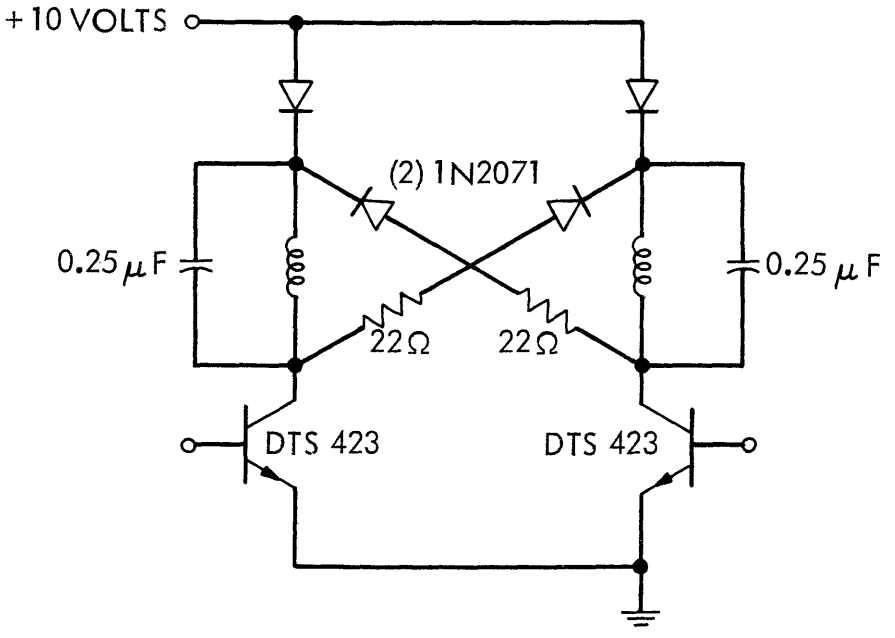

Figure 2.11 Winding Connection for Second Method

proper operation. Therefore, the maximum pulsing frequency is given by $f_{max} = \frac{1}{T_{min}} = 2000$ pps. However, due to the strong mutual coupling between the windings, the large induced voltages at turn-off had opposing effects in the coupled winding and the maximum pulsing rate was only approximately 200 pps. Also, this scheme is very inefficient due to the power dissipating nature of the resistor.

A second scheme, designed and developed by Professor George C. Newton, Jr., would allow for switching transients of approximately 0.3 milliseconds. Thus the maximum pulsing rate could be extended to approximately 2000 pps. Also, due to the method of storing all the magnetic energy, this technique was highly efficient.

The method had the two coupled windings connected as shown in Fig. 2.11. In this way the high induced voltage spikes (180 volts) at the time of switching caused current in the coupled winding to build up to full value in a fraction of a millisecond, the current in one winding being transferred to the other. However, the test results showed that this scheme also failed to increase the maximum pulsing rate, since the mutual coupling in the windings cancelled the effect of the high induced voltages.

The final design suggested by Professor Newton provides a method of compensating the mutual coupling by keeping the induced voltages low (approximately 70 volts) and still reducing the current transients to a fraction of a millisecond. The circuit design is shown in Fig. 2.9 and Fig. 2.12. The major drawback to this design is the extra number of components used, since separate circuits were used for improving the current rise and decay transients.

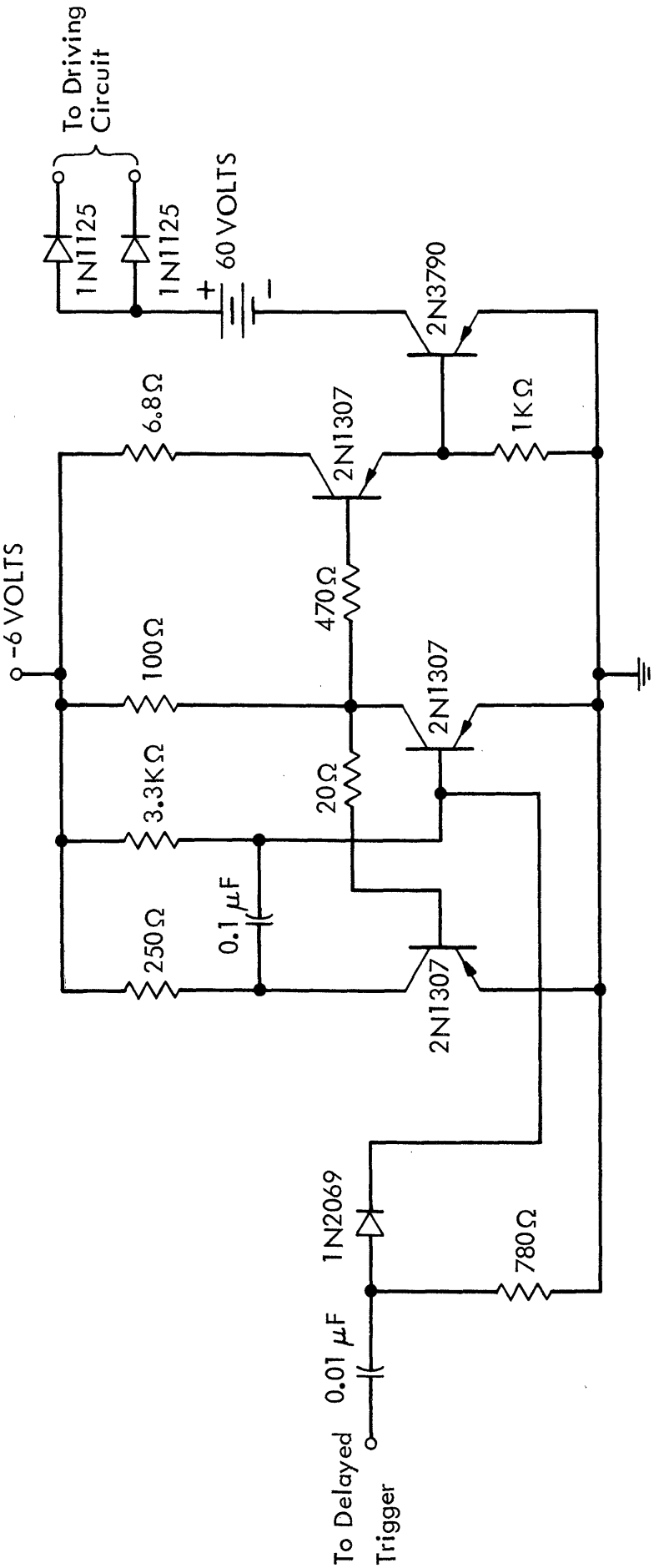

Figure 2.12 Spiking Circuit

The turn-off circuit or feedback path was designed with specific consideration for the mutual coupling. That is, the voltage induced across the winding when the DTS 423 power switch opens was limited to a value of 70 volts. (Thus the opposition due to coupling was greatly reduced from either of the other two designs.) With the Zener diode in the feedback circuit, as shown, the induced voltage is clamped to the Zener voltage once current is shunted through it at turn-off. Also, this voltage remains constant during the entire decay period, since the Zener diode is not turned off until the current through it is down to 1 μa.[6]

However, since Zener diodes with the power and current capabilities required by this application are expensive, the power transistor Motorola 2N1542[6] was used to shunt most of the current through it and thus dissipate most of the power. In this way the voltage across the coil is still clamped to the Zener voltage during the decay transient and thus the rate of current decay is preserved. Since the turn-off current for the Zener diode is low, the gain of the transistor is not critical. If the turn-off current was a milliampere, a high gain transistor would limit the amount of stored energy dissipated during the decay period.

The initial consideration in this design was the decay period. Since pulsing rates of 1000 pps were desired, 0.5 msec was chosen as a safe estimate for the decay transient time. Neglecting the small resistance in the winding, the Zener voltage during this time is equal to the induced voltage $L\frac{di}{dt}$. Here $\Delta I = 1.25$ and $\Delta T = 0.5$ msec. Therefore, the Zener voltage was calculated to be 75 volts. The Motorola 1N3001,[6] chosen for this application, has a test current rating of 37 ma and a Zener voltage of 68 volts. The power requirements estimate,

given by $\frac{\Delta E}{\Delta T} = \frac{1/2\ LI^2}{\Delta T}$, is 30 watts. The Zener diode is rated at 10 watts. However, the Motorola 2N1542 transistor had a minimum current gain of 50 and power capability of 106 watts. Thus the transistor handled most of the current and power dissipation.

This shunt path reduces the current decay time. However, there is still a 3 msec lag in current rise time, due to the winding inductance. In order to reduce this lag, the spiking circuit shown in Fig. 2.12 is used.

This circuit was designed neglecting the mutual coupling effect. Its operation is simply to spike the windings with high voltage for a short period of time with each input pulse. The on time for this operation is determined by the monostable period.

With a 60 volt supply the steady-state current in the coil would be more than 6 amps. However, the idea is to design the period of the monostable such that steady-state is never reached and these excessive currents do not occur. The desired result is to have the winding current reach its full rated current while driven by the 60 volt supply. Since the transient build-up of current is determined by the L/R ratio of the winding (neglecting mutual coupling) the period of the monostable was easily calculated. However, since only a single starting circuitry arrangement was used and there is an overlapping of the "on" times of two of the windings, the current was only allowed to reach half rated value during each driving period of the 60 volt supply. The value is 0.6 amps and using a straignt-line approximation for the first instants of time of the exponential current rise, the time required for current to build up to this value was calculated to be 0.25 msec. This determined the period of the monostable. The interstaging circuitry provided the proper amplification to drive the power transistor 2N3790[6] to

saturation. However, since the windings were coupled it was necessary to delay the monostable trigger in order to isolate the transients. This will be explained in Chapter III.

CHAPTER III

EXPERIMENTAL RESULTS

3.1 INTRODUCTION

For the final circuit described in Chapter II, the desired voltage and current waveforms are shown in Fig. 3.1. However, before the results were obtained experimentally, it was necessary to change some of the circuitry at first. The initial design included only a single feedback path for all four motor windings. Since there was an overlapping of the "on" times of two of the uncoupled windings, the induced voltage when one winding was turned off was transferred through the "on" winding and extra voltage spikes were observed in the V_{CE} waveform. This problem was eliminated by having a turn-off path for each coupled pair of windings.

Secondly, the system was very noise sensitive and the motor response was irregular. This problem was eliminated by making sure all the equipment and circuitry had a common ground.

3.2 VOLTAGE WAVEFORMS

Shown in Fig. 3.2* are the DTS 423 collector voltage waveforms and the voltage across the Zener diode. These agree very well with the calculations and desired waveforms. Zener voltage is 65 volts and the current decay period is 0.5 msec. If the time scale is expanded, it is possible to verify the relation between the Zener voltage and current

---

* In all the experimental waveforms, time goes from right to left.

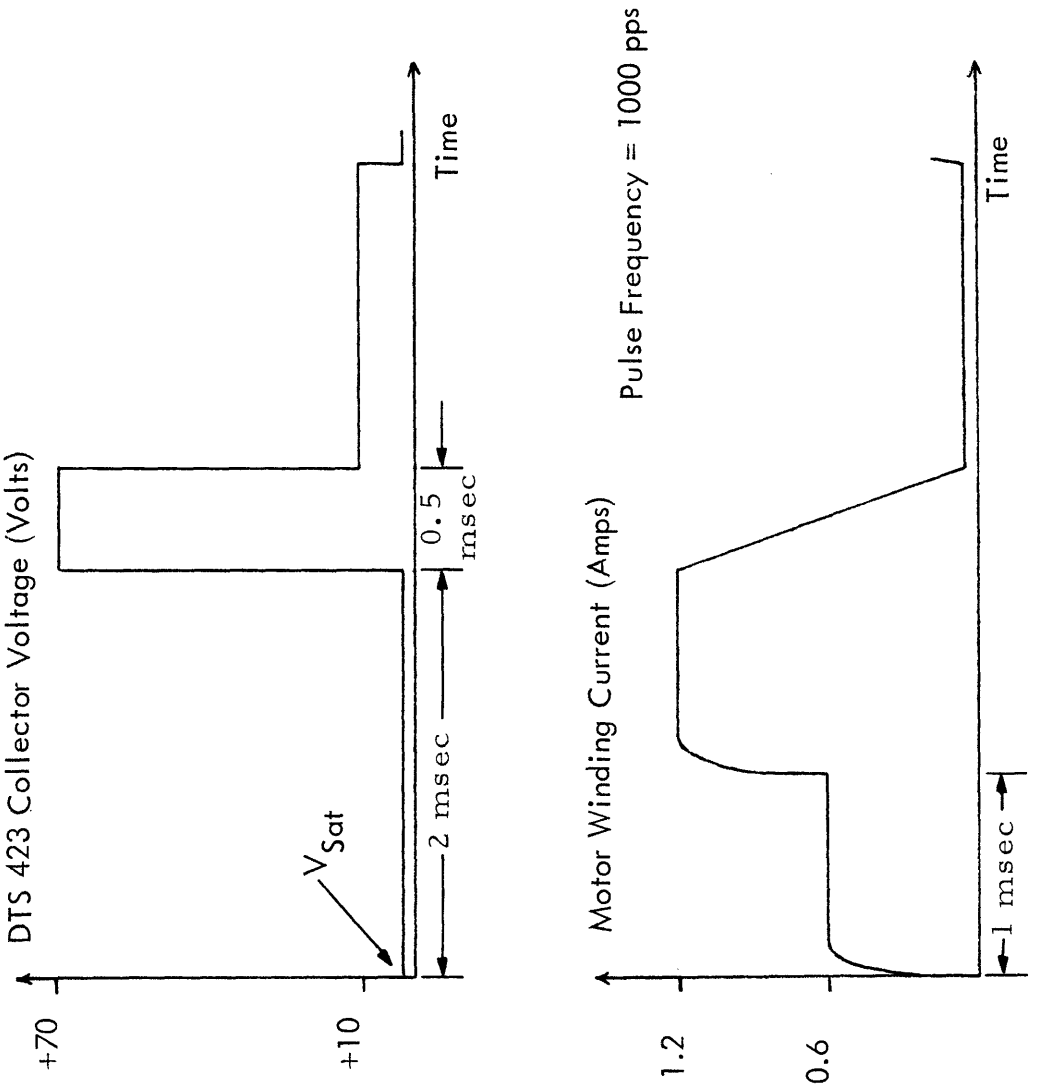

Figure 3.1 Ideal Waveforms

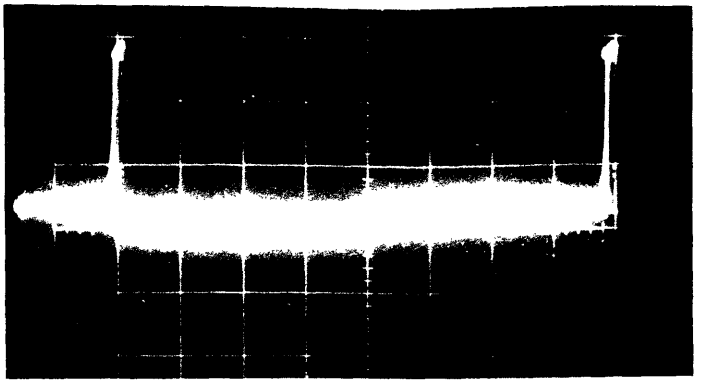

Figure 3.2a Collector Voltage (DTS 423)
Time Base: 2.5 msec/cm
Amplitude Scale: 50 volt/cm

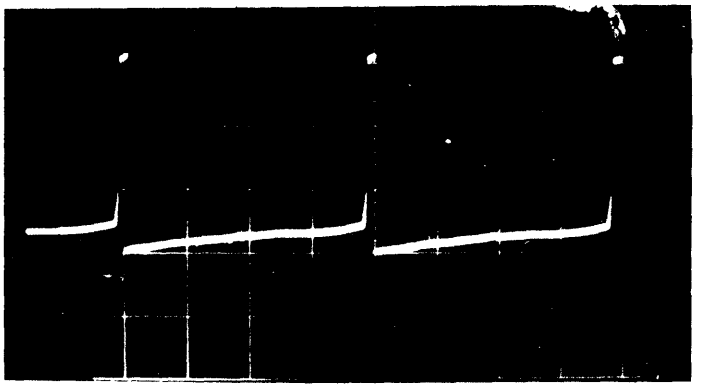

Figure 3.2b Zener Diode Voltage
Time Base: 2.5 msec/cm
Amplitude Scale: 20 volt/cm

decay time. As the pulsing frequency is increased, the current does not reach its maximum value. As a result, the decay transient period is decreased since $L \frac{di}{dt}$ is clamped to the Zener voltage during this time. This effect occurred at approximately 200 pps with the spiking circuit disconnected.

3.3 CURRENT WAVEFORMS

The current waveforms were taken using a 0.41 ohm resistor in series with one of the motor windings. Two features were demonstrated successfully by these waveforms: (1) the effect of mutual coupling on current values and (2) the current waveshape with the spiking circuit engaged. Figure 3.3 is a sequence of traces taken to show the improvement in current rise time using the spiking circuit. These traces were taken with only one pair of windings energized and at a pulsing rate above that to which the rotor could respond. In this way the rotor was locked in and the effect of the mechanical lag could be neglected.

Without the spiking circuit, the equivalent circuit for the "on" time of the winding is a series inductor-resistor circuit. Therefore, the current has an exponential build-up as shown in Fig. 3.3a. At this frequency (approximately 400 pps), the current has time to reach 70 percent of its rated value. With the spiking circuit engaged, the current waveform is changed according to Fig. 3.3b. This agrees with the desired waveform shown in Fig. 3.1. The current nearly reached its rated value due to the two jumps in value during the spiking periods.

Finally, Fig. 3.3c shows the coupling effect. With the coupled winding connected, the current values are reduced. This is due to the fact that during the initial spiking period the mutual inductance effect, as

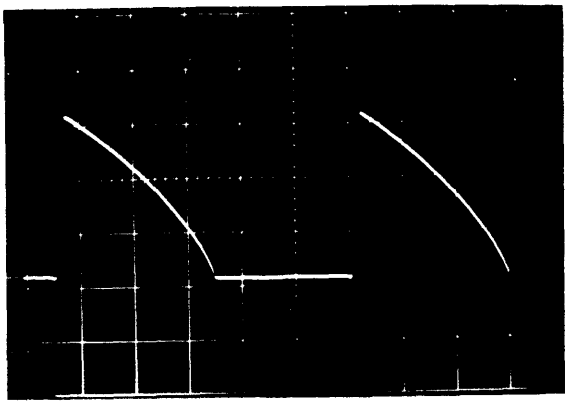

Figure 3.3a Winding Current (Coupled winding Open-circuited; spiking circuit disconnected)
Time Base: 2.0 msec/cm
Amplitude Scale: 0.25 amp/cm

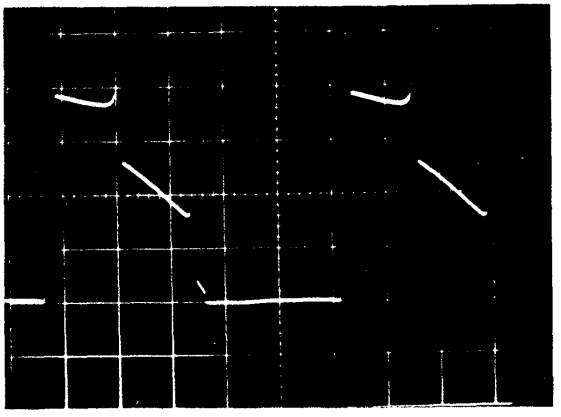

Figure 3.3b Winding Current (Coupled winding Open-circuited; spiking circuit connected)
Time Base: 2.0 msec/cm
Amplitude Scale: 0.25 amp/cm

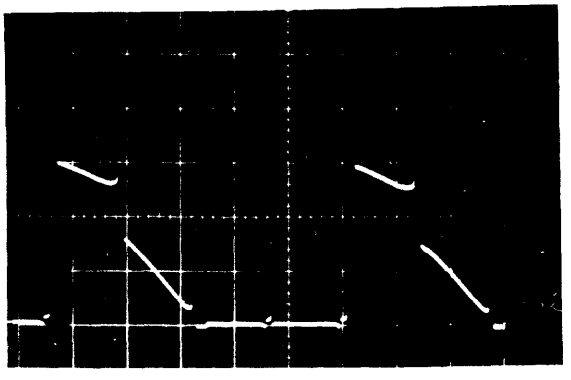

Figure 3.3c Winding Current (Coupled winding connected; spiking circuit connected)
Time Base: 2.0 msec/cm
Amplitude Scale: 0.25 amp/cm

well as the decay transient in the coupled winding, cause a reduced value in the current jump. During the second spiking period, the coupled winding is effectively open-circuited and thus the value of the current rise is preserved. This is to be explained more fully in Chapter IV.

Although the current waveforms were achieved experimentally, the maximum pulsing rate was not increased over the rated value of 200 pps for this stepping motor. Two modifications were required in the spiking circuit operation before the maximum pulsing rate was increased. As mentioned in Chapter II, the actual spiking operation was triggered from the input pulses through a 0.45 msec delay.[7] With this delay, the current in the one winding had enough time to decay before the spike of voltage was applied to the other coupled winding. Otherwise, with overlapping transients, the spiking effect would be cancelled due to the strong coupling between the windings. The waveforms with this new scheme are shown in Fig. 3.4.

Also, at low and intermediate frequencies, the large voltage spikes cause the motor to operate irregularly since the current in the winding during the spiking period was incompatible with the rotor position. Therefore, it was necessary to have a frequency control on the value of the spiking voltage, so that maximum voltage was not applied until the motor was stepping at a very fast rate.

This design was tested and the desired results were achieved within the limitations of the motor design. That is, this circuitry did reduce the electrical lag so that the maximum pulsing rate was increased from 200 pps to 450 pps. However, any further substantial increase is impossible due to the mechanical lag in the motor as well as the increasing opposition due to coupling. This will be explained in Chapter IV.

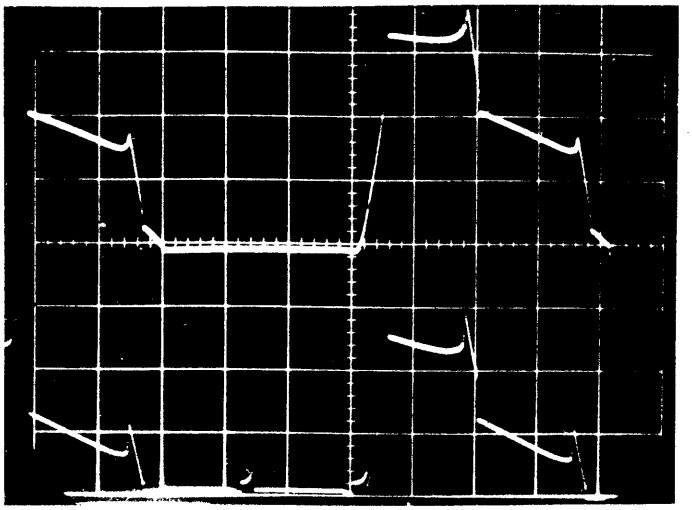

Figure 3.4a Winding Current (Spiking circuit delayed; uncoupled windings open-circuited)
Top: Coupled Winding Open-circuited
Bottom: Coupled Winding Connected
Time Base: 1.0 msec/cm
Amplitude Scale: 0.25 amp/cm

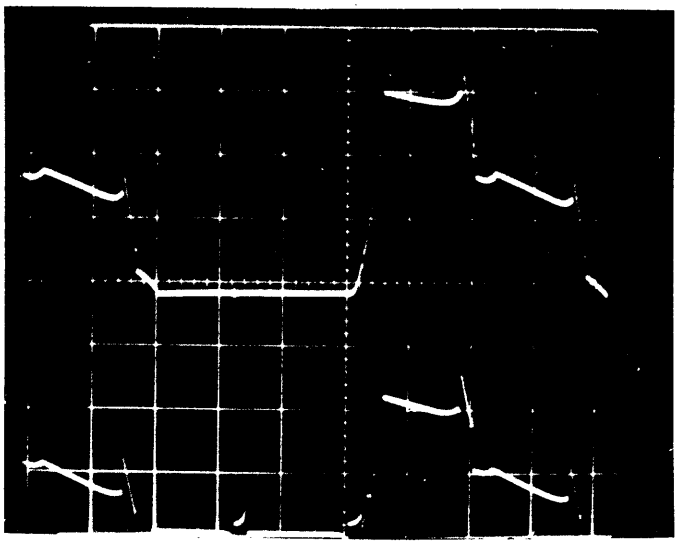

Figure 3.4b Winding Current (Spiking circuit delayed; uncoupled windings engaged)
Top: Coupled Winding Open-Circuited
Bottom: Coupled Winding Connected
Time Base: 1.0 msec/cm
Amplitude Scale: 0.25 amp/cm

CHAPTER IV

ANALYSIS AND CONCLUSIONS

4.1 PURPOSE

The purpose of this experimentation was to extend the maximum pulsing rate of the motor. In general, the time response of the device is limited by both electrical and mechanical parameters. However, the attempt was to reduce only the current transients caused by the inductances of the windings, neglecting any limitations due to the mechanical parameters. This was accomplished by the special driving scheme explained in Chapter II (see section 2.5).

Without this driving circuit, the current turn-on transient is exponential with $\tau = \frac{L}{R}$ = 5 millisec. This is verified by the current trace in Fig. 3.3a. As pulsing period (T) approaches this value, the current does not reach full value and the motor locks in. This corresponds to a frequency of 200 pps ($f = \frac{1}{T} = \frac{1}{\tau}$). By reducing the transients with the special driving scheme, the maximum pulsing rate can be increased, since current will have time to reach full value. The driving circuit was designed to reduce the transients to 0.5 millisec. Theoretically, the maximum pulsing rate could be extended to 2000 pps. However, due to the mutual coupling and mechanical parameters, the maximum pulsing rate was only 450 pps. These effects will now be analyzed and discussed.

4.2 MUTUAL COUPLING EFFECT

Basically, Faraday's Law states that for any change in the magnetic flux through a coil, an emf is induced to oppose this change.[8] This is given

by the relation

$$e = \frac{d\lambda}{dt}$$

e = emf

λ = instantaneous value of flux linkage

t = time

According to Lenz's Law, the direction of the counter emf is such to induce a current which would prevent the flux from changing. Using this principle in transformer analysis, where one or more electric circuits are coupled through a single magnetic field, it is possible to develop an analytical expression for the mutual coupling between two electric circuits. It is this type of mutual coupling which limited the desired results of this research.

Figure 4.1 shows schematically a transformer having two windings on a common magnetic core. The winding currents are i_1 and i_2. According to Faraday's Law, $e_1 = \frac{d\lambda_1}{dt}$ and $e_2 = \frac{d\lambda_2}{dt}$. The leakage flux can be neglected and thus the principle of superposition applied to the flux linkages gives the relations[8]

$$\lambda_1 = N_1 \phi_{m_1} + N_1 \phi_{m_2}$$

$$\lambda_2 = N_2 \phi_{m_2} + N_2 \phi_{m_1}$$

where ϕ_{m_1} is the mutual flux due to current in winding number 1 and ϕ_{m_2} is mutual flux due to current in winding number 2. N_1 and N_2 are the number of turns for each winding, respectively.

Also, self-inductance is defined as the flux linkage with a winding per ampere of current in the same winding. Therefore

$$L_{11} = \frac{N_1 \phi_{m_1}}{i_1}, \quad L_{22} = \frac{N_2 \phi_{m_2}}{i_2}$$

Similarly, mutual inductance is the flux linkage due to an ampere of current in the other winding. Therefore

$$L_{12} = \frac{N_1 \phi_{m_2}}{i_2}, \quad L_{21} = \frac{N_2 \phi_{m_1}}{i_1}$$

Therefore the induced voltages can now be expressed conveniently in terms of currents and inductances.

$$e_1 = \frac{d\lambda_1}{dt} = \frac{d}{dt}(L_{11} i_1 + L_{12} i_2)$$

$$e_2 = \frac{d\lambda_2}{dt} = \frac{d}{dt}(L_{12} i_1 + L_{22} i_2)$$

In these equations, mutual coupling is dependent only on the geometry of the system and therefore, $L_{12} = L_{21}$. For static coupled circuits, the inductances are constant. Therefore:

$$v_1 = r_1 i_1 + L_{11} \frac{di_1}{dt} + L_{12} \frac{di_2}{dt}$$

$$v_2 = r_2 i_2 + L_{22} \frac{di_2}{dt} + L_{12} \frac{di_1}{dt}$$

Thus for coupled circuits, Faraday's Law results in an additional term in the basic circuit equation. The magnitude of this term is dependent on the amount of coupling (L_{12}) and it either opposes or aids the transient behavior in the coupled circuit.

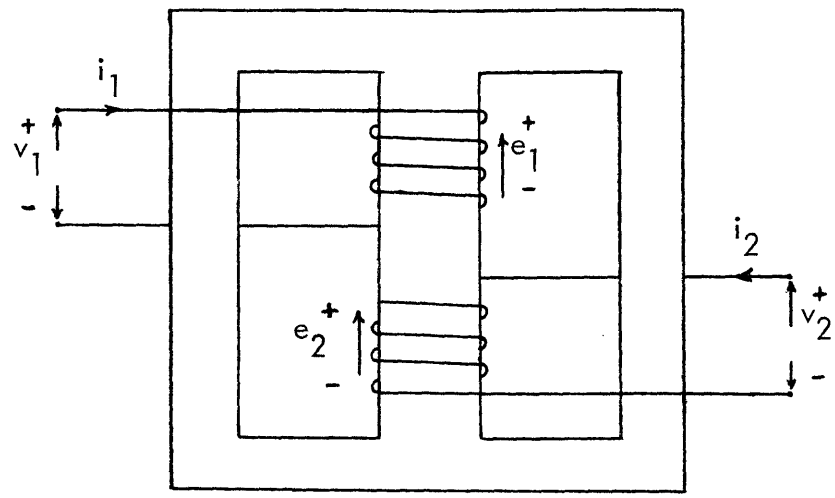

Figure 4.1 Schematic Diagram of Transformer

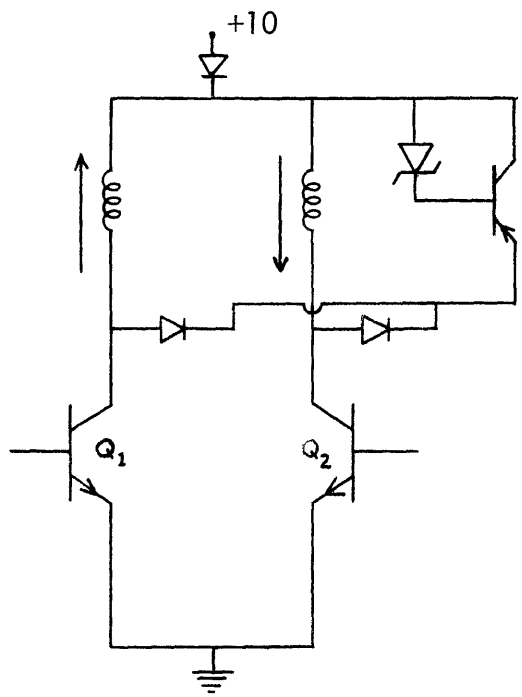

Figure 4.2 Connection for Pair of Coupled Windings

The Slo-Syn motor SS150 has bifilar windings. Each pair of windings, formed by center-tapping the two windings, is coupled since they are wound on the same poles, only in opposite directions. Following the theory developed, any change in the flux due to current change in one coil induces an emf in the coupled winding. According to Faraday's Law, this induced emf opposes the change in flux. However, whether it opposes the desired current transient depends on how the coils are wound.

Figure 4.2 shows the basic connection for the motor's coupled pair of windings. This pair of windings experiences on-off excitation explained in Chapter II. That is, as Q_1 is turned off, Q_2 is turned on. The flux paths for full current in each winding are also shown in the diagram. With no coupling between the windings, the current in winding number 1 would decay and the current of winding number 2 would build up, the transient times determined by the special driving scheme discussed in Chapter II. However, with coupling between the windings, the current decay in winding number 1 causes current to flow in winding number 2 in a direction opposing the decrease in flux caused by the change in winding number 1 current. Since this current flow is in the direction opposite that of the flux path shown for current in winding number 2, it opposes the current rise in winding number 2. This is a reciprocal effect. Therefore, transient improvements are limited by the induced voltages caused by coupling.

This effect is demonstrated in the voltage and current waveforms shown in Chapter III. In Fig. 3.2 the voltage measured from the collector of the power transistor to ground is approximately twice the Zener voltage during the turn-off transient. This corresponds to the induced voltage due to the change in current plus the Zener voltage due to the actual current flow.

In Fig. 4.3, the coupling causes large spikes of voltage during the off part of the current cycle. This is due to the spiking circuit driving the coupled winding as well as the rotor motion, both of which cause induced effects in the winding. Also, all the current traces in Chapter III show a reduction in current magnitude when the coupled winding is connected. The coupling actually only effects the current change during the first spiking period, since there is no coupling between the "on" winding and the one turned on at the 1/2 cycle point.

The best way to overcome the coupling problem is by isolating current transients. This was done by delaying the trigger in the spiking circuit. However, the coupling can never be eliminated so that any attempt to speed up current transients increases the opposition to current flow in the coupled winding. Thus the performance of the designed circuit was limited by this phenomenon.

It is well to note that the measured value of the mutual coupling between the center-tapped winding halves was approximately 100 percent. This was measured using a low-signal sinusoidal source on the primary and measuring the output across the coupled winding, both short-circuited and open-circuited. This verifies the decrease in current magnitude that occurs when the coupled winding is connected, (see Figs. 3.3 and 3.4).

4.3 MECHANICAL PARAMETERS

Secondly, another limitation to the desired time response was due to the mechanical lag inherent in the motor. Originally this effect was neglected, since it was assumed that the rotor inertia was low and the holding torque provided by the permanent magnet strong enough so that the lag was not a limitation on the desired response. However, this is

Figure 4.3 Winding Current (Motor Running at Approximately 450 pps)

Time Base: 1.0 msec/cm

Amplitude Scale: 0.25 amp/cm

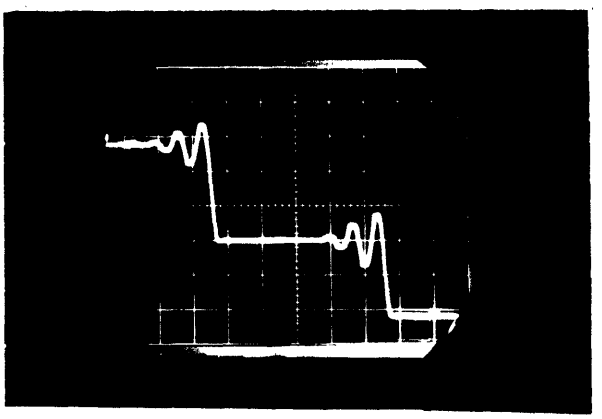

Figure 4.4 Angular Output at 50 pps

Time Base: 4.0 msec/cm

Amplitude Scale: 0.8°/cm

not the case which will now be demonstrated.

As mentioned above, the Slo-Syn stepping motor behaves like a second-order, closed-loop positioning system during a single step. Its step response is shown in Fig. 4.4. Here the oscillations are due to inertial loading and the holding torque provides the damping. The differential equation governing this response is given by [9]

$$T_{DEV} = J\frac{d^2\theta}{dt^2} + B\frac{d\theta}{dt} + K\theta$$

T_{DEV} = Electromagnetic torque

J = Rotor inertia

B = Rotor damping

K = Spring constant

θ = Rotor position

In order for the motor to stop and start without error, these transient oscillations should have settled before another input pulse is applied. The motor appears to stay synchronized until the pulsing rate increases to the point where the time interval between pulses is comparable to the build-up time τ_B of the above second-order system response. This build-up time τ_B is measured to be 2.4 msec. Therefore, the pulsing frequency has an approximate upper bound given by

$$f_{max} = \frac{10^3}{2.4} = 410 \text{ pps}$$

This agrees with the experimental results for the maximum pulsing frequency and explains why the desired frequency of 2000 pps was not achieved.

Further, this explains the unusual form of the current trace in Fig. 4.3. The torque developed is a complicated function of field excitation and geometry. Since it is a nonlinear system, it is very difficult to obtain an analytical expression for this torque. However, a simplified model will suffice to demonstrate the principle. For a two-field, linear system the general torque expression is

$$T_{DEV} = T_{MAX} \sin \psi$$

ψ = torque angle (angle between the two fields)

T_{MAX} = maximum torque

Consider a four-position stepping motor with two fields, one the stator field and the other due to a permanent magnet rotor. The torque vs position for a single excitation period is shown in Fig. 4.5.[1]

With no load torque all the towque developed goes into acceleration. At low frequencies, the permanent magnet aligns itself with the stator field during each step. Therefore, maximum torque is developed at the beginning of each step since $\psi = 90^{\circ}$. However, at high frequencies, the rotor does not have sufficient time to align and thus maximum torque is not developed initially, thereby reducing the acceleration capability.

In the current traces, it is this lag in rotor position, due to the mechanical parameters, which causes the unusual waveform. The above explanation of coupling was based on static conditions. However, with motion there are induced voltages associated with angular velocity. At high frequencies, these voltages cause increased opposition to current flow in the coupled winding. Therefore, at approximately 450 pps, the current decreases once the special spiking circuit is disconnected.

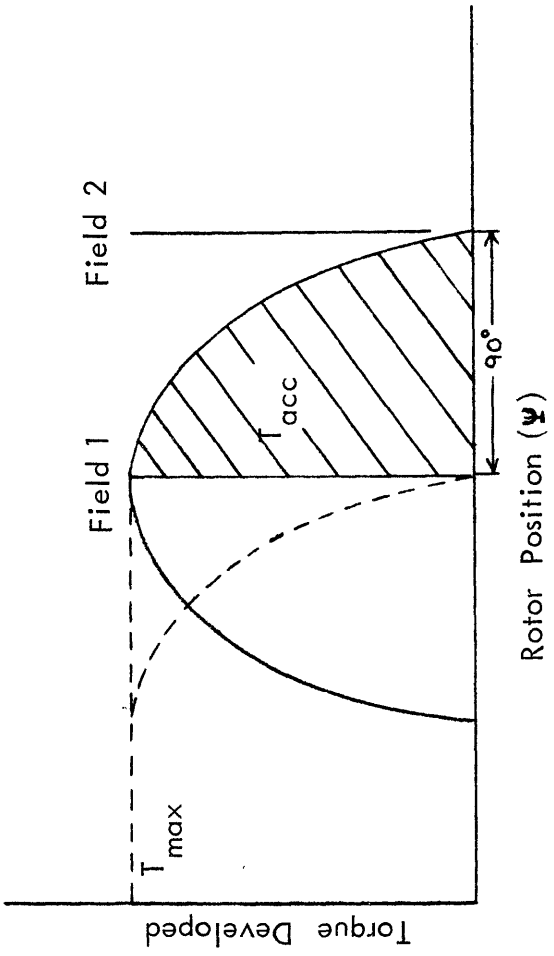

Figure 4.5 Torque vs Position for no Load

The conclusion is that both speed limitations for the motor must be considered: that due to the motor design and that due to the limitations of the control circuit. This is a case of the motor design limiting high speed performance.

4.4 FURTHER RESEARCH

The rated current for the motor is 1.25 amp. The special driving circuitry was designed for operating the motor at this value. However, the current traces indicated that this maximum value was not attained. It would be worthwhile to investigate whether this limitation can be improved by increasing the power supply voltage. The results could be compared with those already obtained to verify whether the speed limitation is due to mechanical effects alone.

Also, an alternate scheme would be to use separate spiking circuits for each coupled pair of windings so current would be full on - off rather than the step waveform achieved by this design. This would give a more exact measurement of the mutual coupling. Also, the electrical lag in this situation could be neglected in the response relative to the mechanical lag.

Since the system is nonlinear, direct analysis is very complicated. However, using the nonuniform pulsing logic and reversing logic already explained, it would be possible to measure the output torque as well as evaluate the mechanical parameters. Donald Western[10] proposed a method for measuring torque. It consists of reversing the motor every input pulse and increasing the motor excitation until the motor skips a pulse. The torque is indicated by a calibrated torsion bar. With the pulse

packet logic, the mechanical parameters can be evaluated by varying the inertial loading and the pulsing frequency and counting the number of pulses gained or missed per revolution.

REFERENCES

1. Morraele, A. P., "Theory and Operation of Step-Servo Motors," Electrical Design News; July, 1963.

2. Bailey, S. J., "Incremental Servos - I: Stepping vs Stepless Control," Control Engineering, Vol. 7, No. 11, page 123; November, 1960.

3. Snowden, A. E., Madsen, E. W., "Characteristics of a Synchronous Induction Motor," AIEE Transactions, Part II, Application and Industry, Vol. 81, pages 1 - 5; March, 1962.

4. Baty, G., "Stepper Motors," Electromechanical Design, Vol. 10, No. 7; July, 1966.

5. Proctor, J., "Stepping Motors Move In," Product Engineering, Vol. 34, No. 3, pages 74-88; February 4, 1963.

6. Motorola, Semiconductor Data Manual; 1965.

7. Millman, J., Taub, H., Pulse, Digital, and Switching Waveforms, McGraw-Hill, Inc.,; 1965.

8. Fitzgerals, A. E., Kingsley, C., Electric Machinery, Chapter 1, McGraw-Hill, Inc.; 1961.

9. Kuo, B. C., Automatic Control Systems, Prentice-Hall, Inc., Englewood Cliffs, New Jersey,; 1962, Chapter 4.

10. Western, D., "Characterization and Application of a Responsyn Stepping Motor," M. S. Thesis, M.I.T.; 1966.